Neuropsychopharmacology (2011) 36, 2650–2658

www.neuropsychopharmacology.org

Astrocytic Hypertrophy in Anterior Cingulate White Matter of Depressed Suicides

Susana G Torres-Platas[1,3], Christa Hercher[1,3], Maria Antonietta Davoli[1], Gilles Maussion[1], Benoit Labonté[1], Gustavo Turecki[1,2] and Naguib Mechawar*[,1,2]

[1]McGill Group for Suicide Studies, Department of Neurology and Neurosurgery, Douglas Mental Health University Institute, McGill University, Verdun, Québec, Canada; [2]McGill Group for Suicide Studies, Department of Psychiatry, Douglas Mental Health University Institute, McGill University, Verdun, Québec, Canada

Increasing evidence suggests that cortical astrocytic function is disrupted in mood disorders and suicide. The fine neuroanatomy of astrocytes, however, remains to be investigated in these psychiatric conditions. In this study, we performed a detailed morphometric analysis of 3D-reconstructed gray and white matter astrocytes in Golgi-impregnated anterior cingulate cortex (ACC) samples from depressed suicides and matched controls. Postmortem ACC samples (BA24) from 10 well-characterized depressed suicides and 10 matched sudden-death controls were obtained from the Quebec Suicide Brain Bank. Golgi-impregnated protoplasmic astrocytes (gray matter, layer VI) and fibrous astrocytes (adjacent white matter) were reconstructed, and their morphometric features were analyzed using the Neurolucida software. For each cell, the soma size as well as the number, length, and branching of processes were determined. The densities of thorny protrusions found along the processes of both astrocytic subtypes were also determined. Protoplasmic astrocytes showed no significant difference between groups for any of the quantified parameters. However, fibrous astrocytes had significantly larger cell bodies, as well as longer, more ramified processes in depressed suicides, with values for these parameters being about twice as high as those measured in controls. These results provide the first evidence of altered cortical astrocytic morphology in mood disorders. The presence of hypertrophic astrocytes in BA24 white matter is consistent with reports suggesting white matter alterations in depression, and provides further support to the neuroinflammatory theory of depression.
Neuropsychopharmacology (2011) **36,** 2650–2658; doi:10.1038/npp.2011.154; published online 3 August 2011

Keywords: depression; suicide; limbic; cerebral cortex; glia; inflammation

INTRODUCTION

Mood disorders affect more than 20 million adults per year in the United States alone (Kessler *et al*, 2005). These often severe conditions result too frequently in suicide completion, with psychological autopsy studies indicating that at least 40% of all adult suicides have had a previous diagnosis of depression or bipolar disorder (BPD) (Arsenault-Lapierre *et al*, 2004). Furthermore, up to 15% of individuals with a lifetime diagnosis of major depressive disorder (MDD) (Chen and Dilsaver, 1996) and 50% of individuals with BPD have a history of attempted suicide (Jamison, 2000).

In the search for biological factors underlying depression, neuroanatomical investigations of fronto-limbic cortical circuitries have suggested altered densities and distribution patterns of glial cells (Ongür *et al*, 1998; Rajkowska *et al*, 1999; reviewed by Cotter *et al*, 2001; Hercher *et al*, 2009b), although other studies have not reached the same conclusions (Bouras *et al*, 2001; Hercher *et al*, 2009a). Unfortunately, all of these studies are limited by the fact that they are based on a simple discrimination of neurons and glia according to differences in cresyl violet staining of the cytoplasm and nucleus, and thus cannot account for changes in specific glial cell subpopulations. Work focused on the specific astrocytic marker glial fibrillary acidic protein (GFAP) (Miguel-Hidalgo *et al*, 2000; Si *et al*, 2004) and on the excitatory amino-acid transporters (EAAT1–2) (Miguel-Hidalgo *et al*, 2010) has suggested that cortical astrocytic function may be perturbed in depression. Moreover, expression of the astrocyte-specific tropomyosin-related kinase-B receptor (TrkB.1) isoform and of astrocyte connexins 30 and 43 was recently found to be down-regulated, respectively, in the orbitofrontal cortex and the

*Correspondence: Dr N Mechawar, McGill Group for Suicide Studies, Department of Psychiatry, Douglas Mental Health University Institute, McGill University, 6875 LaSalle Blvd, Verdun, Montreal, Canada, Quebec H4H 1R3, Tel: +514 761 6131 (ext. 3365), Fax: +514 888 4064, E-mail: naguib.mechawar@mcgill.ca
[3]These authors contributed equally to this work.
Received 26 April 2011; revised 29 June 2011; accepted 5 July 2011

dorsolateral prefrontal cortex of suicide completers (Ernst *et al*, 2009, 2011). Taken together, these studies lend support to the hypothesis that communication within cortical astrocytic networks is affected in mood disorders, and are consistent with neuroimaging evidence indicating that both structure and function of fronto-limbic cortical areas are altered in mood disorders (Drevets *et al*, 2008). Indeed, astrocytes provide crucial metabolic support to neuronal networks in the CNS (Allaman *et al*, 2010), and their activity is a major determinant of fMRI signals (Prior *et al*, 2004; Schummers *et al*, 2008; Sibson *et al*, 2008). Furthermore, it is now well established that astrocytes are directly involved in many facets of neuronal function, such as neurotransmission and neuroplasticity (Allaman *et al*, 2010; Araque, 2008; Auld and Robitaille, 2003; Fellin, 2009). By assembling in syncytial networks through gap junctions, astrocytes are also well positioned to rapidly convey information within and between brain regions (Cornell-Bell and Finkbeiner, 1991; Goldberg *et al*, 2010).

Largely on the basis of fine anatomical criteria, two main subtypes of cortical astrocytes have been traditionally recognized in mammals: protoplasmic and fibrous astrocytes, residing in the gray and white matter, respectively. However, recent work conducted by Oberheim *et al* (2009) has revealed a greater diversity and complexity of cortical astrocytes in humans. Human astrocytes were found to be proportionally larger and their processes more elaborate than in rodents. Furthermore, these investigators described a cortical astrocytic subtype unique to man, the 'varicose' astrocyte, which can project a single varicose process across several cortical columns (Oberheim *et al*, 2009). The physiology of cortical astrocytes in humans also shows distinctive features, namely propagation of fast intracellular calcium waves (Oberheim *et al*, 2009). Despite these recent advances, little is known about the fine morphological features of cortical astrocytes in humans, and nothing in the context of psychiatric disorders. The major aim of this study was to conduct comparative morphometric analyses of protoplasmic and fibrous astrocytes in Golgi-stained postmortem anterior cingulate cortex (ACC) samples from depressed suicides and matched non-psychiatric controls. Our working hypothesis was that astrocytes would show altered features in depressed suicides, in line with the putative disorganization of cortical astrocytic networks in mood disorders.

SUBJECTS AND METHODS

Subjects

This study was approved by the Douglas Hospital Research Ethics Board, and written informed consent from next-of-kin was obtained for each subject. Postmortem brain samples from depressed suicides ($n = 10$) and matched sudden-death controls ($n = 10$) were provided by the Quebec Suicide Brain Bank (www.douglasrecherche.qc.ca/suicide). All psychiatric subjects committed suicide in the context of a major depressive episode (see Table 1 for diagnosis distribution), and controls died suddenly without any psychiatric or neurological illness. For each individual, the cause of death was ascertained by the Quebec Coroner's Office, and psychological autopsies were performed by proxy-based interviews, as described previously (Dumais *et al*, 2005). In brief, a trained interviewer conducted the Structured Clinical Interview for DSM-IV Psychiatric Disorders (SCID-I) with one or more informants of the deceased, after which a panel of clinicians reviewed SCID-I assessments, case reports, Coroner's notes, and medical records to obtain consensus psychiatric diagnosis. The subject groups were matched for age ($p = 0.97$), tissue pH ($p = 0.26$), tissue storage time ($p = 0.71$), and postmortem interval (PMI; $p = 0.13$). Furthermore, the delay between death and refrigeration of the bodies at the morgue was also matched between groups (averages of 8.82 and 10.97 h for depressed suicides and controls, respectively; $p = 0.481$).

Table 1 Subject information

	Controls ($n = 10$)	Depressed suicides ($n = 10$)
	Mean ± SEM	Mean ± SEM
Age (years)	48.3 ± 5.9	48.6 ± 5.3
Gender	8M:2F	7M:3F
Tissue pH	6.5 ± 0.13	6.6 ± 0.5
PMI (h)	57.0 ± 5.7	41.0 ± 6.4
Cause of death	5 cardiovascular	7 hanging
	3 road accident	2 intoxication
	2 falling	1 jumping
Clinical information		
Unipolar depression	—	7
Bipolar depression	—	3
Smoking	3	4
Alcohol dependence	—	4
Antidepressants	—	7 (1)*

*Presence of antidepressants was only detected by toxicological analysis in 1/7 subjects.

Golgi Impregnation

Formalin-fixed ACC samples (1 cm^3) adjacent to the dorsal part of the genu of the corpus callosum (BA24) (Gittins and Harrison, 2004; Vogt *et al*, 1995) were dissected from the right hemisphere and silver-impregnated according to a modified Golgi protocol described previously (Hercher *et al*, 2010). Briefly, tissue blocks were processed separately, in the dark and in constant agitation at room temperature. Samples were first immersed in a solution of 3% $K_2Cr_2O_7$ and 10% formalin for 24 h, followed by 24 h in a fresh solution of 3% $K_2Cr_2O_7$, then washed in distilled water and in 2% $AgNO_3$ until the solution ran transparent. Samples were next placed in 2% $AgNO_3$ for 48 h before being dehydrated through a graded series of ethanol solutions, cleared in xylene, embedded in paraffin, and cut on a microtome into serial 50 μm-thick sections.

Morphometric Analyses

All samples were coded and analyzed randomly by a researcher blinded to subject number and diagnosis. A total

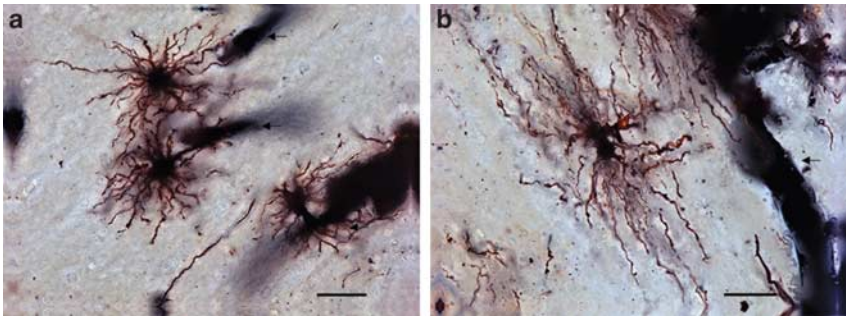

Figure 1 Representative examples of Golgi-stained protoplasmic and fibrous astrocytes in the human ACC. In the gray matter layer VI, protoplasmic astrocytes from a control subject (a) showed a characteristic spherical cell body, with tortuous varicose and thorny processes radiating in all directions. Fibrous astrocyte in the white matter (b) of the same subject presented a more oblong cell body, with relatively long and unramified varicose and thorny processes extended mainly in two opposite directions. Micrographs taken at three different focal points were merged to produce the image in panel b. Processes extended by both astrocytic subtypes were often seen contacting blood vessels (arrows). Scale bar = (a): 10 μm; (b): 25 μm.

of 200 astrocytes were reconstructed and analyzed in this study. For each subject, five protoplasmic astrocytes were analyzed in the gray matter and five fibrous astrocytes in the white matter. Data acquired for each cell population were averaged per subject. Owing to the greater diversity of astrocytic subtypes in the upper cortical layers and the higher density of astrocytes in the lower cortical layers (Miguel-Hidalgo *et al*, 2000; Oberheim *et al*, 2009; Oberheim *et al*, 2006), protoplasmic astrocytes were selected exclusively from layer VI. When scanning through randomly selected subsets of serial sections, using random observational patterns, the first five astrocytes encountered per layer (ie, layer VI or white matter) that fulfilled the following criteria were selected for analysis: (1) Location of the cell body in lower layer VI or in adjacent white matter, for protoplasmic and fibrous astrocytes, respectively; (2) full impregnation of the cell body and its processes; (3) astrocytic processes unobscured by background staining or by other cells; and (4) characteristic bushy morphology for protoplasmic astrocytes (layer VI) and presence of relatively unbranched processes for fibrous astrocytes (white matter) (Figure 1). In addition, the great majority of selected cells were readily observed to contact blood vessels, a canonical attribute of astrocytes (Figure 1).

Astrocytes were traced under a $\times 100$ (NA 1.40) oil immersion objective (Olympus BX51 light microscope) and their processes were analyzed in three dimensions within single sections by using a computer-based tracing system (Neurolucida v. 8.10.2; MBF Bioscience, Williston, VT) (Figure 2). Only cell bodies were analyzed in two dimensions (area at its largest cross-sectional diameter) because of limitations associated with tracing and measuring Golgi-stained somas in three dimensions with this software. Thus, for each astrocyte, the cell body area as well as the number, length, diameter, and branching points (nodes) of its processes were measured. We further observed thorny protrusions along the length of processes extended by all protoplasmic and fibrous astrocyte (Figure 3). These structures were similar in appearance to dendritic spines, with an approximate length of 0.5–1.5 μm. The density of these protrusions was also determined for each astrocytic process and expressed as numbers of astrocytic spines per micrometer. In order to further assess the spatial distribution of astrocytic processes, a 3D version of the Sholl analysis (Sholl, 1956) was used. In this analysis, a series of increasing 10-μm concentric circles around the soma allowed the quantification of the distribution of each parameter within a given radius, and thus in relation to the cell body.

Statistical Analyses

Statistical analyses were performed by using PASW Statistics 18 (Statistical Product and Service Solutions, Chicago, IL, USA). All measurements were expressed as mean ± SEM and $p \leqslant 0.05$ was considered significant in all statistical tests. Normality was assessed by using Shapiro–Wilk tests and parametric between-subject two-tailed *t*-tests were applied for normally distributed data sets. Two-tailed *U*-tests were used for non-normally distributed data. For Sholl analyses, two-way, mixed-design, between-subject (controls/depressed suicides) and within-subject (distance from cell body) ANOVAs were performed. This was followed by simple effects test to determine specific points of statistical significance. Multiple correlation analyses followed by ANCOVAs were used to examine the influence on measured variables of potential confounders. The latter comprised age, PMI, brain pH, tissue storage time, medication use, alcohol dependence, and smoking.

RESULTS

Cell Body Size

No significant difference was found between layer VI protoplasmic astrocytes in controls ($110.3 \pm 11.5\,\mu m^2$) and in depressed suicides ($134.6 \pm 21.1\,\mu m^2$) (Figure 4a). However, the cell body size of white matter fibrous astrocytes was significantly larger in depressed suicides ($150.7 \pm 11.6\,\mu m^2$) than in controls ($114.5 \pm 10\,\mu m^2$) ($t_{(18)} = -2.319$, $p = 0.032$) (Figure 4b).

Astrocytic Processes

The number of primary processes radiating from the cell body did not differ between depressed suicides and controls for either protoplasmic astrocytes (13.6 ± 0.7 *vs* 14.7 ± 0.5 processes, respectively) or fibrous astrocytes (19.8 ± 1.0 *vs* 19.1 ± 1.1 processes, respectively). Similarly, branching of these primary processes was similar between depressed

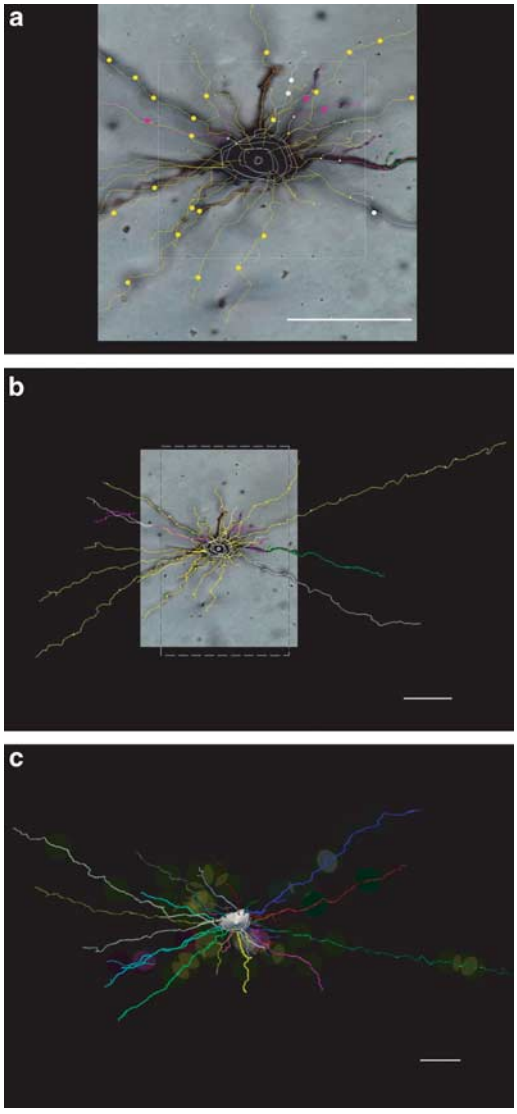

Figure 2 3D reconstruction of processes extended by astrocytes. Reconstructing processes extended by astrocytes and visualized across the depth of histological sections with the Neurolucida software involved several steps that are summarized here in the case of a BA24 white matter fibrous astrocyte. The image in panel b is a lower magnification of the one shown in panel a. First, the outline of the cell body is traced at its largest cross-sectional diameter to measure its area. For the purpose of this illustration, the soma outline was drawn at different focal points to generate a 3D image. Second, the course of each process was tracked and traced along its full length within the tissue section, as shown by colored segments extended by the cell body (a, b). Color codes were used to identify primary and higher-order branches, and markers (eg, small circles), to label particular features such as astrocytic spines or nodes. The reconstructed cell is shown in (c), with each primary process and its branches coded by a different color. Scale bar = 25 μm.

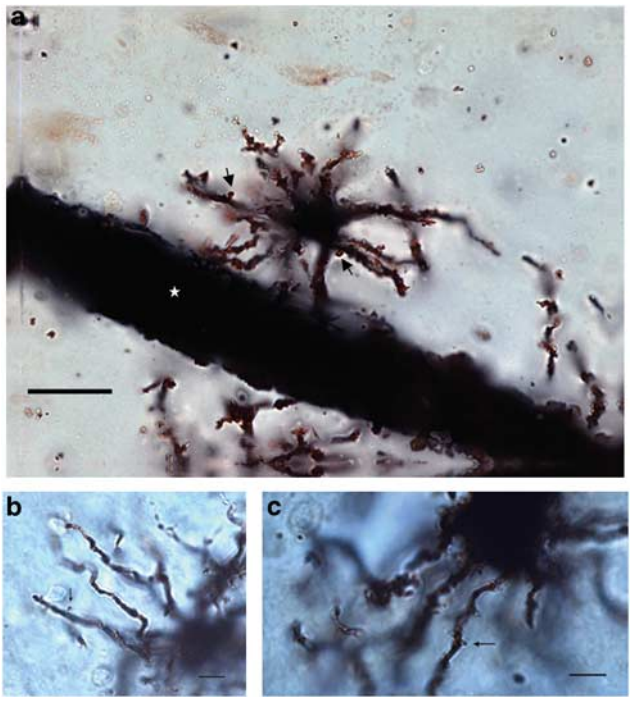

Figure 3 Spines are a feature of protoplasmic and fibrous astrocytic processes in the human ACC. Golgi-stained astrocytic processes were always observed to be thorny. This was due to the presence of spine-like structures (black arrows) found along processes extended by protoplasmic (a) and fibrous astrocytes (b, c) alike. Micrographs taken at three different focal points were merged to produce the image in panel a. Several processes of the protoplasmic astrocytes illustrated in panel a contact a large blood vessel (white star). Scale bars = (a): 10 μm; (b, c): 25 μm.

suicides and controls in the case of gray matter protoplasmic astrocytes, with very similar numbers of branch ends (33.2 ± 2.2 *vs* 34.4 ± 2.7 ends, respectively) and nodes (18.6 ± 1.6 *vs* 18.6 ± 2.3 nodes, respectively) (Figure 5a). By contrast, white matter fibrous astrocytes showed a highly significant, more than twofold, increase in average number of nodes in depressed suicides as compared with controls (39.8 ± 4.0 *vs* 18.3 ± 1.9 nodes, respectively) ($t_{(18)} = -4.644$, $p = 0.0002$) (Figure 5b). As expected, the average number of branch ends was also significantly increased in fibrous astrocytes (63.3 ± 4.9 *vs* 39.0 ± 2.8 ends, respectively) ($t_{(18)} = -4.268$, $p = 0.0004$). To evaluate the effect of this increased branching on the length of processes, total branch length was then measured and found to be similar between protoplasmic astrocytes in depressed suicides and controls (697.3 ± 50.0 *vs* 717.1 ± 59.3 μm, respectively) (Figure 6a), but significantly increased in fibrous astrocytes of depressed suicides as compared with controls (1557.0 ± 174.0 *vs* 797.1 ± 129.0 μm, respectively) ($t_{(18)} = -3.493$, $p = 0.002$) (Figure 6b). The average length of processes (total length divided by number of primary processes) projected by protoplasmic astrocytes was consequently similar between depressed suicides and controls (52.3 ± 2.4 *vs* 49.6 ± 3.8 μm, respectively), but increased significantly for fibrous astrocytes in the former group (80.2 ± 9.3 *vs* 41.2 ± 5.3 m, respectively) ($t_{(18)} = -3.625$, $p = 0.001$). Similarly, the total volume of processes per astrocyte was on average significantly higher in depressed suicides as compared with controls for fibrous astrocytes (1111.8 ± 99.7 *vs* $576.3 \pm 41.8\ \mu m^3$, respectively) ($t_{(18)} = -4.953$, $p = 0.0001$) but not for protoplasmic astrocytes (1159.1 ± 235.8 *vs* $1121.9 \pm 400.8\ \mu m^3$, respectively).

Astrocytic Spines

On average, the total number of spines per protoplasmic astrocyte was similar between depressed suicides and

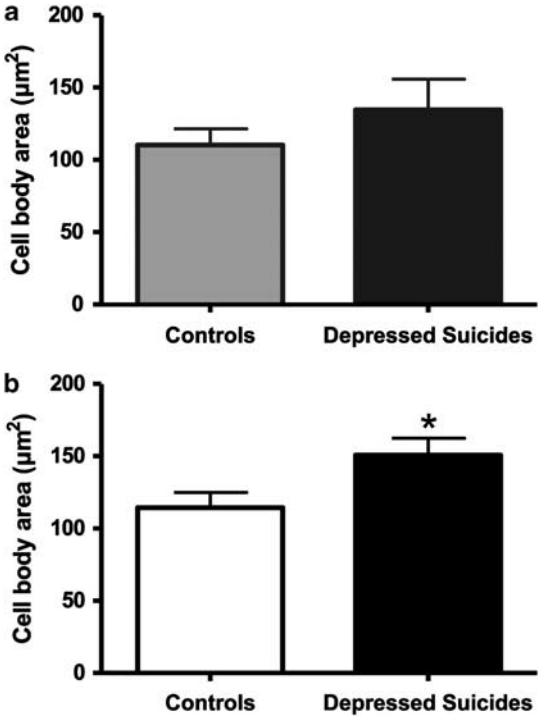

Figure 4 Fibrous astrocytes in BA24 of depressed suicides present a significantly larger cell body area than in controls. Both layer VI protoplasmic (a) and white matter fibrous (b) astrocytes showed a greater cell body area in depressed suicides than in matched controls. However, this increased soma size was significant only in the case of fibrous astrocytes. *$p < 0.05$.

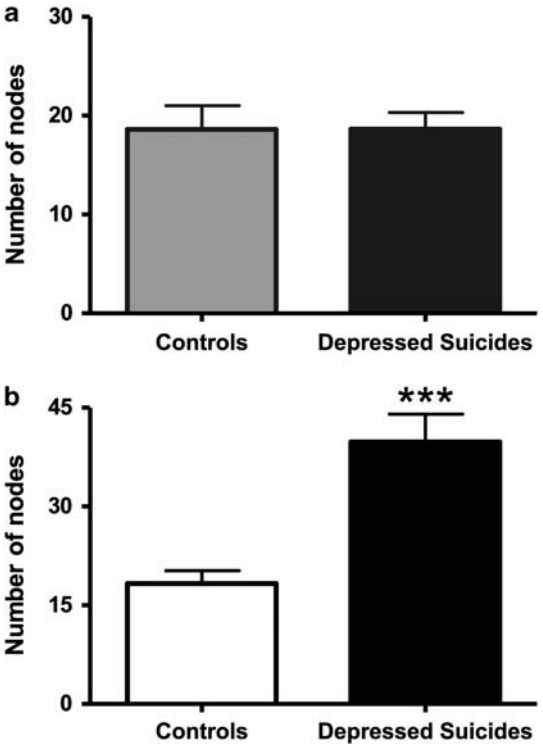

Figure 5 Fibrous astrocytes in BA24 of depressed suicides present significantly more branching points than in controls. The number of nodes made by processes was similar between groups for layer VI protoplasmic astrocytes (a) but more than twice higher in depressed suicides in the case of fibrous astrocytes (b). ***$p < 0.0005$.

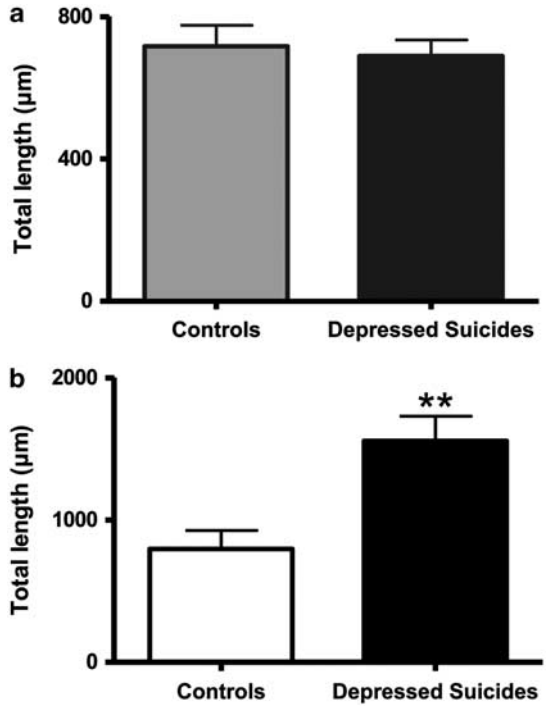

Figure 6 Fibrous astrocyte projections in BA24 are significantly longer in depressed suicides than in matched controls. The numbers of processes emerging from the cell body were found to be similar between groups for both protoplasmic and fibrous astrocytes (see Results). However, the total length of processes per cell was significantly different between groups in the case of fibrous astrocytes, with a value almost twice as high in depressed suicides than in controls (b). As expected, with an absence of group difference in the number of nodes per cell, total process length was very similar between groups for protoplasmic astrocytes (a). **$p < 0.005$.

controls (21.8 ± 3.9 *vs* 22.1 ± 2.7 spines, respectively) (Figure 7a), but significantly higher for fibrous astrocytes in depressed suicides (57.3 ± 16.0 *vs* 20.5 ± 3.8 spines, respectively; $p = 0.003$) ($U_{(18)} = 80$, $p = 0.023$) (Figure 7b). This likely resulted from the increased process length per cell in the latter group, as supported by the fact that the density of spines borne by astrocytic processes did not differ between groups for protoplasmic astrocytes (0.035 ± 0.006 *vs* 0.034 ± 0.007 spines per μm) or fibrous astrocytes (0.034 ± 0.008 *vs* 0.027 ± 0.004 spines per μm) in depressed suicides as compared with controls, respectively.

Sholl Analyses

The following parameters were quantified by Sholl analysis: length and volume of processes, intersections, nodes, and astrocytic spines. As expected from the data presented above, Sholl analyses did not reveal any significant difference in any of these parameters when comparing layer VI protoplasmic astrocytes in depressed suicides and controls (not shown). The measured increase in process length per white matter fibrous astrocyte in depressed suicides was also evidenced by Sholl analysis, in terms of number of intersections, number of nodes, as well as process length. Thus, compared with fibrous astrocytes in controls, increases in process volume and process length (Figure 8) were highly significant in all radii between 20 and

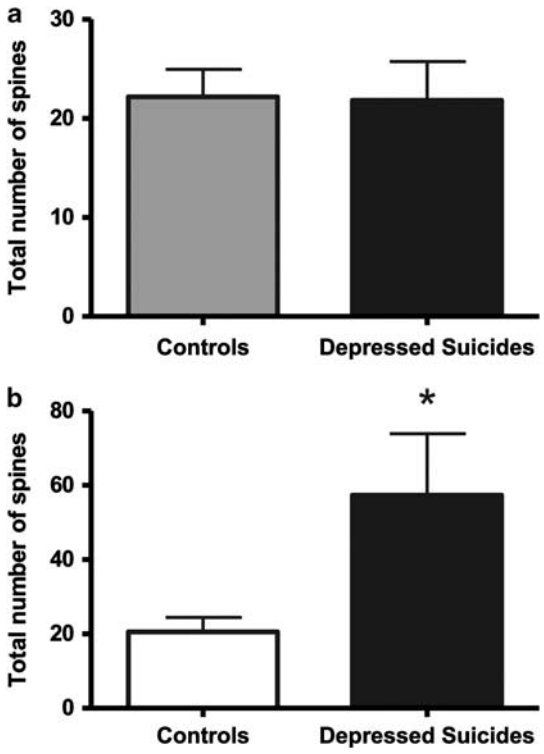

Figure 7 Astrocytic spines in fibrous astrocytes are significantly increased in depressed suicides owing to the increase in process length per cell. The density of spines per process length was similar for both astrocytic subtypes and did not present any group differences (see Results). In relation to total process length per cell, however, the total number of spines per cell was significantly higher in depressed suicides as compared with controls in the case of fibrous (b) but not protoplasmic astrocytes (a). $*p<0.05$.

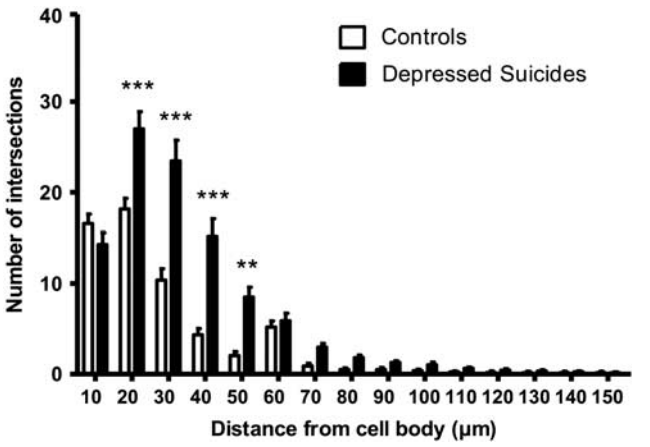

Figure 8 Sholl analysis of intersections made by processes of fibrous astrocytes. Sholl analysis confirmed that process length and branching pattern of fibrous astrocytes are more elaborate in depressed suicides than in controls, with increased intersections being found within almost all concentric radii between 20 and 50 μm around the cell body. $**p<0.005$, $***p<0.0005$.

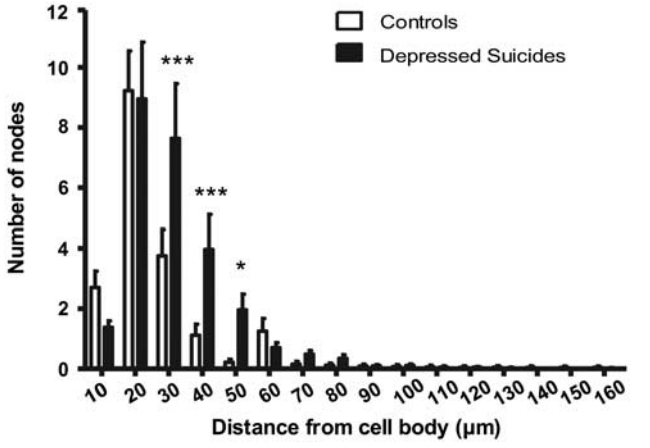

Figure 9 Sholl analysis of branching points shown by fibrous astrocytic processes. Sholl analysis revealed that the higher number of nodes shown by fibrous astrocytes in depressed suicides as compared with controls was mainly localized at 30, 40, and 50 μm away from the cell body. $*p<0.05$, $***p<0.0005$.

50 μm ($p<0.005$). Furthermore, intersections and nodes formed by fibrous astrocytes in depressed suicides were significantly more numerous than in controls between 30 and 50 μm away from the soma ($p<0.022$; Figure 9). Finally, more astrocytic spines were generally found between 30 and 50 μm from the fibrous astrocyte soma in depressed suicides as compared with controls ($p<0.012$; Figure 10).

Potential Confounders

None of the potential confounders was found to influence any of the measured variables significantly.

Taken together, these data reveal that fibrous astrocytes in BA24 white matter present hypertrophic features in depressed suicides as compared with controls (Figure 11).

DISCUSSION

This is the first postmortem study to provide a detailed fine neuroanatomical assessment of cortical astrocytes in both healthy and psychiatric subjects. Morphometric analyses confirmed the complex arborization patterns shown by human protoplasmic and fibrous astrocytes (Oberheim *et al*, 2009). Despite clear differences (eg, branching patterns), many similarities were found between these two astrocytic subtypes. One of the common features was the presence, along processes, of protrusions reminiscent of dendritic spines. Thorny processes were recently mentioned as a feature of protoplasmic astrocytes in the human temporal cortex (Oberheim *et al*, 2009). Here, we show that thorny processes are also characteristic of fibrous astrocytes, and that their density along processes is similar in both astrocytic subtypes. We currently ignore the functional role of these spines, which, to our knowledge, have never been described in other species, but it is tempting to speculate that they represent specialized postsynaptic structures analogous to dendritic spines. Future work using electron microscopy will be required to gain a better understanding of their ultrastructural features and microenvironment.

A major finding of this study arose from the comparison of BA24 astrocytes in depressed suicides and matched

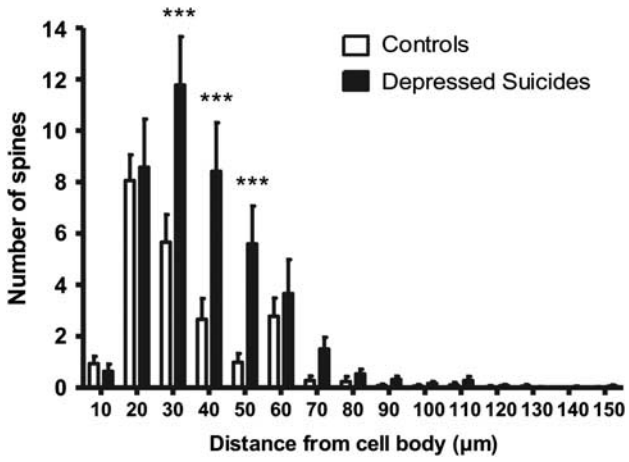

Figure 10 Sholl analysis of spine numbers shown by fibrous astrocytic processes. Sholl analysis revealed that the higher number of spines shown by fibrous astrocytes in depressed suicides compared with controls was mainly localized between 30 and 60 μm away from the cell body. ***$p < 0.0005$.

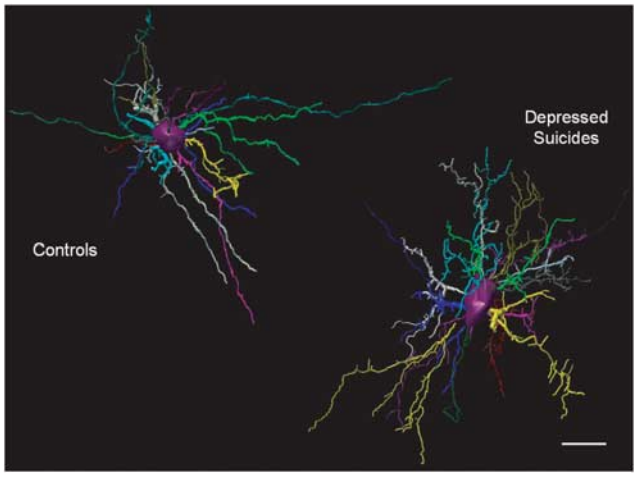

Figure 11 Fibrous astrocytes are hypertrophic in BA24 white matter of depressed suicides. 3D reconstructions of representative BA24 fibrous astrocytes in controls and depressed suicides. As illustrated, fibrous astrocytes in the latter group show larger cell bodies and increased branching and length of their processes. Scale bar = 25 μm.

controls. Although the morphometric features of protoplasmic astrocytes were in all points comparable between groups, fibrous astrocytes were found to be larger and to extend longer and more ramified processes in depressed suicides (Figure 11). These results further highlight the distinctiveness of astrocytic subtypes within the same cortical region, and suggest that a morphological remodeling may occur in fibrous astrocytes independently of adjacent gray matter protoplasmic astrocytes. Importantly, this is the first report of selective cellular changes occurring in the white matter in depression. Alterations in the ACC white matter circuitry are likely to impact on communication between this cortical area and other intimately associated brain regions implicated in depression, such as the amygdala and the prefrontal cortex (Allman *et al*, 2001; Vogt *et al*, 1995).

The cortical area investigated here was described previously by our group to show similar Nissl-stained (upper and lower cortical) glial densities in young adult depressed suicides as compared with controls (Hercher *et al*, 2009b). Interestingly, in an elegant quantitative analysis published by Miguel-Hidalgo *et al* (2000), the packing density and areal fraction occupied by GFAP-immunoreactive astrocytes in the dorsolateral prefrontal cortex were found to differ between MDD subjects and matched controls, but only when younger (30–45 years old) and older (46–86 years old) subjects were considered independently. A subsequent study by the same group showed a strongly significant positive correlation between GFAP protein levels and age at time of death in depressed subjects (Si *et al*, 2004). Furthermore, GFAP protein levels were also found to be positively correlated with the areal fraction occupied by GFAP-immunoreactivity in BA9 (Si *et al*, 2004). The results of the present study, showing similar anatomical features between BA24 protoplasmic astrocytes in middle-aged depressed suicides and matched controls, suggest that if alterations in GFAP expression also occur in this region in depressed suicides, they are not accompanied by morphological changes. However, this does not preclude the possibility that astrocytic function and signaling are affected in depression and suicide, as suggested previously (Ernst *et al*, 2009, 2011; Miguel-Hidalgo *et al*, 2000, 2010; Si *et al*, 2004).

It can be hypothesized that the hypertrophic fibrous astrocytes described here in depressed suicides reflect local inflammation in the white matter. Strong lines of evidence support the neuroinflammatory theory of depression (Maes *et al*, 2009). In particular, it has been well documented that patients suffering from depression have significantly higher levels of circulating pro-inflammatory cytokines (Miller *et al*, 2009), and that administration of interferon-α leads to depressive-like symptoms (Malaguarnera *et al*, 1998; reviewed by Horsmans, 2006) that are accompanied by increased ACC activation (Capuron *et al*, 2005). Expression of brain cytokines seems altered in suicides (Tonelli *et al*, 2008), and pro-inflammatory cytokines have been implicated in the development of stress-induced depressive symptoms (Audet *et al*, 2010; Goshen *et al*, 2008). The differences between cortical gray and white matter astrocytes highlighted in the present study need to be explored further, but may have to do with an increased facility of cytokines to diffuse within the brain along white matter tracts (Konsman *et al*, 2000). Interestingly, white matter hyper-intensities (WMHs) (Debette and Markus, 2010), which are thought to represent regions of acute astrocyte activation (Simpson *et al*, 2007) or astrogliosis (Fazekas *et al*, 1993), increase the risk of developing MDD (Bae *et al*, 2006; de Groot *et al*, 2000; Iosifescu *et al*, 2007; Li *et al*, 2007; reviewed by Tham *et al*, 2010) and are strongly associated with suicide (Grangeon *et al*, 2010). WMHs, have been proposed to arise from inflammation and oxidative stress (Wright *et al*, 2009; Xu *et al*, 2010; reviewed by Rosenberg, 2009) both of which are well documented to be increased in depression (Maes, 2008; Miller *et al*, 2009).

When interpreting the results of this study, two particular limitations need to be kept in mind. First, given that the

reconstruction and morphometric analysis of each astrocyte constituted a lengthy and labor-intensive process, the sample size was relatively modest (20 subjects, 200 cells). Multiple correlation analyses followed by ANCOVAs were performed to evaluate the influence on measured variables of potential confounders such as alcohol dependence, smoking, and medication. Although none of these factors were found to influence any of the variables significantly, it is acknowledged that the statistical power to detect such confounders was somewhat limited owing to sample size. Nevertheless, the specificity and statistical significance of the findings are reassuring. Second, we cannot establish whether our observations are due to depression, suicide, or to a combination both. Future work could clarify this issue by including samples from non-depressed suicides and depressed non-suicides.

In summary, this first morphometric characterization of human cortical gray and white matter astrocytes shows unexpected features such as spines, found along processes extended by both protoplasmic and fibrous astrocytes. It also reveals highly significant morphological changes displayed by BA24 white matter fibrous astrocytes in depressed suicides as compared with controls. These changes, which were not found in adjacent layer VI protoplasmic astrocytes, consisted of larger cell bodies as well as longer and more ramified processes. Taken together, these results suggest significant differences between ACC cortical gray and white matter astrocytic activation that may reflect a state of chronic inflammation affecting the white matter compartment of this limbic region in depression and suicide.

ACKNOWLEDGEMENTS

We acknowledge the precious collaboration of the Quebec Coroner's Office, as well as the cooperation and support of the next-of-kin of the deceased. We also thank the expert staff of the Quebec Suicide Brain Bank, which is funded in part by the Réseau Québécois de Recherche sur le Suicide (FRSQ). Ruth Sawicki, Lilian Canetti, Marissa Maheu, and Volodymyr Yerko are thanked for technical assistance, Dr Gregory Dal Bo for his helpful advice, and Dr Joseph Rochford for statistical expertise. This work was funded by operating grants from CIHR (NM) and FRSQ (NM and GT), as well as an infrastructure grant from CFI (NM), and an equipment grant from NSERC (NM). SGTP is the recipient of a CONACYT PhD scholarship and NM is an FRSQ scholar.

DISCLOSURE

All authors declare no conflict of interest.

REFERENCES

Allaman I, Belanger M, Magistretti PJ (2010). Astrocyte–neuron metabolic relationships: for better and for worse. *Trends Neurosci* **34**: 76–87.

Allman JM, Hakeem A, Erwin JM, Nimchinsky E, Hof P (2001). The anterior cingulate cortex. The evolution of an interface between emotion and cognition. *Ann NY Acad Sci* **935**: 107–117.

Araque A (2008). Astrocytes process synaptic information. *Neuron Glia Biol* **4**: 3–10.

Arsenault-Lapierre G, Kim C, Turecki G (2004). Psychiatric diagnoses in 3275 suicides: a meta-analysis. *BMC Psychiatry* **4**: 37.

Audet MC, Mangano EN, Anisman H (2010). Behavior and pro-inflammatory cytokine variations among submissive and dominant mice engaged in aggressive encounters: moderation by corticosterone reactivity. *Front Behav Neurosci* **4**: 156.

Auld DS, Robitaille R (2003). Glial cells and neurotransmission: an inclusive view of synaptic function. *Neuron* **40**: 389–400.

Bae JN, MacFall JR, Krishnan KR, Payne ME, Steffens DC, Taylor WD (2006). Dorsolateral prefrontal cortex and anterior cingulate cortex white matter alterations in late-life depression. *Biol Psychiatry* **60**: 1356–1363.

Bouras C, Kovari E, Hof PR, Riederer BM, Giannakopoulos P (2001). Anterior cingulate cortex pathology in schizophrenia and bipolar disorder. *Acta Neuropathol* **102**: 373–379.

Capuron L, Pagnoni G, Demetrashvili M, Woolwine BJ, Nemeroff CB, Berns GS *et al* (2005). Anterior cingulate activation and error processing during interferon-alpha treatment. *Biol Psychiatry* **58**: 190–196.

Chen YW, Dilsaver SC (1996). Lifetime rates of suicide attempts among subjects with bipolar and unipolar disorders relative to subjects with other Axis I disorders. *Biol Psychiatry* **39**: 896–899.

Cornell-Bell AH, Finkbeiner SM (1991). Ca^{2+} waves in astrocytes. *Cell Calcium* **12**: 185–204.

Cotter DR, Pariante CM, Everall IP (2001). Glial cell abnormalities in major psychiatric disorders: the evidence and implications. *Brain Res Bull* **55**: 585–595.

de Groot JC, de Leeuw FE, Oudkerk M, Hofman A, Jolles J, Breteler MM (2000). Cerebral white matter lesions and depressive symptoms in elderly adults. *Arch Gen Psychiatry* **57**: 1071–1076.

Debette S, Markus HS (2010). The clinical importance of white matter hyperintensities on brain magnetic resonance imaging: systematic review and meta-analysis. *BMJ* **341**: c3666.

Drevets WC, Price JL, Furey ML (2008). Brain structural and functional abnormalities in mood disorders: implications for neurocircuitry models of depression. *Brain Struct Funct* **213**: 93–118.

Dumais A, Lesage AD, Alda M, Rouleau G, Dumont M, Chawky N *et al* (2005). Risk factors for suicide completion in major depression: a case-control study of impulsive and aggressive behaviors in men. *Am J Psychiatry* **162**: 2116–2124.

Ernst C, Deleva V, Deng X, Sequeira A, Pomarenski A, Klempan T *et al* (2009). Alternative splicing, methylation state, and expression profile of tropomyosin-related kinase B in the frontal cortex of suicide completers. *Arch Gen Psychiatry* **66**: 22–32.

Ernst C, Nagy C, Yang JP, Deng X, Hellstrom IC, Choi KH *et al* (2011). Dysfuction of astrocyte connexin 30 and 43 in dorsolateral prefrontal cortex of suicide completers. *Biol Psychiatry* **70**: 312–319.

Fazekas F, Kleinert R, Offenbacher H, Schmidt R, Kleinert G, Payer F *et al* (1993). Pathologic correlates of incidental MRI white matter signal hyperintensities. *Neurology* **43**: 1683–1689.

Fellin T (2009). Communication between neurons and astrocytes: relevance to the modulation of synaptic and network activity. *J Neurochem* **108**: 533–544.

Gittins R, Harrison PJ (2004). A quantitative morphometric study of the human anterior cingulate cortex. *Brain Res* **1013**: 212–222.

Goldberg M, De Pitta M, Volman V, Berry H, Ben-Jacob E (2010). Nonlinear gap junctions enable long-distance propagation of pulsating calcium waves in astrocyte networks. *PLoS Comput Biol* **6**: e10000909.

Goshen I, Kreisel T, Ben-Menachem-Zidon O, Licht T, Weidenfeld J, Ben-Hur T *et al* (2008). Brain interleukin-1 mediates chronic stress-induced depression in mice via adrenocortical activation and hippocampal neurogenesis suppression. *Mol Psychiatry* **13**: 717–728.

Grangeon MC, Seixas C, Quarantini LC, Miranda-Scippa A, Pompili M, Steffens DC *et al* (2010). White matter hyperintensities and their association with suicidality in major affective disorders: a meta-analysis of magnetic resonance imaging studies. *CNS Spectr* **15**: 375–381.

Hercher C, Canetti L, Turecki G, Mechawar N (2010). Anterior cingulate pyramidal neurons display altered dendritic branching in depressed suicides. *J Psychiatr Res* **44**: 286–293.

Hercher C, Parent M, Flores C, Canetti L, Turecki G, Mechawar N (2009a). Alcohol dependence-related increase of glial cell density in the anterior cingulate cortex of suicide completers. *J Psychiatry Neurosci* **34**: 281–288.

Hercher C, Turecki G, Mechawar N (2009b). Through the looking glass: examining neuroanatomical evidence for cellular alterations in major depression. *J Psychiatr Res* **43**: 947–961.

Horsmans Y (2006). Interferon-induced depression in chronic hepatitis C. *J Antimicrob Chemother* **58**: 711–713.

Iosifescu DV, Renshaw PF, Dougherty DD, Lyoo IK, Lee HK, Fraguas R *et al* (2007). Major depressive disorder with anger attacks and subcortical MRI white matter hyperintensities. *J Nerv Ment Dis* **195**: 175–178.

Jamison KR (2000). Suicide and bipolar disorder. *J Clin Psychiatry* **61**(Suppl 9): 47–51.

Kessler RC, Chiu WT, Demler O, Merikangas KR, Walters EE (2005). Prevalence, severity, and comorbidity of 12-month DSM-IV disorders in the National Comorbidity Survey Replication. *Arch Gen Psychiatry* **62**: 617–627.

Konsman JP, Tridon V, Dantzer R (2000). Diffusion and action of intracerebroventricularly injected interleukin-1 in the CNS. *Neuroscience* **101**: 957–967.

Li L, Ma N, Li Z, Tan L, Liu J, Gong G *et al* (2007). Prefrontal white matter abnormalities in young adult with major depressive disorder: a diffusion tensor imaging study. *Brain Res* **1168**: 124–128.

Maes M (2008). The cytokine hypothesis of depression: inflammation, oxidative & nitrosative stress (IO&NS) and leaky gut as new targets for adjunctive treatments in depression. *Neuroendocrinol Lett* **29**: 287–291.

Maes M, Yirmyia R, Noraberg J, Brene S, Hibbeln J, Perini G *et al* (2009). The inflammatory & neurodegenerative (I&ND) hypothesis of depression: leads for future research and new drug developments in depression. *Metab Brain Dis* **24**: 27–53.

Malaguarnera M, Di Fazio I, Restuccia S, Pistone G, Ferlito L, Rampello L (1998). Interferon alpha-induced depression in chronic hepatitis C patients: comparison between different types of interferon alpha. *Neuropsychobiology* **37**: 93–97.

Miguel-Hidalgo JJ, Baucom C, Dilley G, Overholser JC, Meltzer HY, Stockmeier CA *et al* (2000). Glial fibrillary acidic protein immunoreactivity in the prefrontal cortex distinguishes younger from older adults in major depressive disorder. *Biol Psychiatry* **48**: 861–873.

Miguel-Hidalgo JJ, Waltzer R, Whittom AA, Austin MC, Rajkowska G, Stockmeier CA (2010). Glial and glutamatergic markers in depression, alcoholism, and their comorbidity. *J Affect Disord* **127**: 230–240.

Miller AH, Maletic V, Raison CL (2009). Inflammation and its discontents: the role of cytokines in the pathophysiology of major depression. *Biol Psychiatry* **65**: 732–741.

Oberheim NA, Takano T, Han X, He W, Lin JH, Wang F *et al* (2009). Uniquely hominid features of adult human astrocytes. *J Neurosci* **29**: 3276–3287.

Oberheim NA, Wang X, Goldman S, Nedergaard M (2006). Astrocytic complexity distinguishes the human brain. *Trends Neurosci* **29**: 547–553.

Ongür D, Drevets WC, Price JL (1998). Glial reduction in the subgenual prefrontal cortex in mood disorders. *Proc Natl Acad Sci USA* **95**: 13290–13295.

Prior MJ, Brown AM, Mavroudis G, Lister T, Ray DE (2004). MRI characterisation of a novel rat model of focal astrocyte loss. *MAGMA* **17**: 125–132.

Rajkowska G, Miguel-Hidalgo JJ, Wei J, Dilley G, Pittman SD, Meltzer HY *et al* (1999). Morphometric evidence for neuronal and glial prefrontal cell pathology in major depression. *Biol Psychiatry* **45**: 1085–1098.

Rosenberg GA (2009). Inflammation and white matter damage in vascular cognitive impairment. *Stroke* **40**(3 Suppl): S20–S23.

Schummers J, Yu H, Sur M (2008). Tuned responses of astrocytes and their influence on hemodynamic signals in the visual cortex. *Science* **320**: 1638–1643.

Sholl DA (1956). The measurable parameters of the cerebral cortex and their significance in its organization. *Prog Neurobiol* **2**: 324–333.

Si X, Miguel-Hidalgo JJ, O'Dwyer G, Stockmeier CA, Rajkowska G (2004). Age-dependent reductions in the level of glial fibrillary acidic protein in the prefrontal cortex in major depression. *Neuropsychopharmacology* **29**: 2088–2096.

Sibson NR, Lowe JP, Blamire AM, Martin MJ, Obrenovitch TP, Anthony DC (2008). Acute astrocyte activation in brain detected by MRI: new insights into T(1) hypointensity. *J Cereb Blood Flow Metab* **28**: 621–632.

Simpson JE, Fernando MS, Clark L, Ince PG, Matthews F, Forster G *et al* (2007). White matter lesions in an unselected cohort of the elderly: astrocytic, microglial and oligodendrocyte precursor cell responses. *Neuropathol Appl Neurobiol* **33**: 410–419.

Tham MW, Woon PS, Sum MY, Lee TS, Sim K (2010). White matter abnormalities in major depression: evidence from post-mortem, neuroimaging and genetic studies. *J Affect Disord* **132**: 26–36.

Tonelli LH, Stiller J, Rujescu D, Giegling I, Schneider B, Maurer K *et al* (2008). Elevated cytokine expression in the orbitofrontal cortex of victims of suicide. *Acta Psychiatr Scand* **117**: 198–206.

Vogt BA, Nimchinsky EA, Vogt LJ, Hof PR (1995). Human cingulate cortex: surface features, flat maps, and cytoarchitecture. *J Comp Neurol* **359**: 490–506.

Wright CB, Moon Y, Paik MC, Brown TR, Rabbani L, Yoshita M *et al* (2009). Inflammatory biomarkers of vascular risk as correlates of leukoariosis. *Stroke* **40**: 3466–3471.

Xu H, Stamova B, Jickling G, Tian Y, Zhan X, Ander BP *et al* (2010). Distinctive RNA expression profiles in blood associated with white matter hyperintensities in brain. *Stroke* **41**: 2744–2749.